AUT Journal of Electrical Engineering

AUT J. Elec. Eng., 56(1) (Special Issue) (2024) 19-36
DOI: 10.22060/eej.2023.21371.5473

Online Non-Intrusive Efficiency Monitoring of Pumping Systems

M. J. Karimi [1], A. Sadighi [2]*

[1] Department of Mechanical Engineering, University of Tehran, Tehran, Iran
[2] School of Mechanical Engineering, University of Tehran, Tehran, Iran

ABSTRACT: Moving toward a sustainable energy future requires improving the efficiency of energy systems. The fact that about 22% of industrial electricity is consumed by induction-motor-driven centrifugal pumps, highlights the importance of continuous monitoring of such systems to ensure they are operating at their best efficiency points. This results in the overall reduction of energy consumption and consequently lowers the carbon footprint of pumping systems. This paper presents a non-intrusive approach towards estimating the efficiency of the whole motor pump chain. The motor efficiency is calculated using only motor electrical signals along with the nameplate information. To estimate the pump efficiency, a hybrid method is adopted which uses the pump characteristic curve, impeller speed, and affinity laws. Both estimation algorithms are based on electrical signature analysis (ESA) which requires only motor terminal quantities i.e. current and voltage. The proposed methods are tested on laboratory setups and the experimental results show their accuracy in estimating the efficiency of induction-motor-driven pumps. Given the non-intrusive nature of the proposed method, a simple data acquisition system to acquire motor current and voltage signals along with a microprocessor to implement the algorithms discussed here can be integrated into a single affordable board to be used in utilities for continuous efficiency monitoring purposes.

Review History:
Received: Oct. 04, 2022
Revised: Apr. 12, 2023
Accepted: Apr. 13, 2023
Available Online: Feb. 01, 2024

Keywords:
Induction motor
centrifugal pump
efficiency estimation
non-intrusive methods
electrical signature analysis

1- Introduction

Using electric motors to drive pumps, fans, and compressors comprises almost 46% of the electric energy consumed in industries[1]. The European Commission mentioned that electric motor applications in pumping systems consumed nearly 22% of this energy [2]. As stated in [3], changing pump system components or applying other flow control techniques can save about 30% of wasted energy. Increased energy prices and environmental issues are the other reasons that highlight the importance of efficiency monitoring in these systems.

The three-phase induction motor and a centrifugal pump are the two main parts of an industrial pumping system. Electric energy converts to mechanical power in the motors and then transforms to hydraulic power in the pump units. To estimate the efficiency of the overall system, some mechanical variables, such as motor speed and its output torque, and some hydraulic variables including pump head and flow rate, are required. However these variables are not always available, and installing related sensors to measure them directly is not a viable solution since these sensors are too costly and decrease the system's reliability.

An increasing number of studies have been published for three-phase induction motor efficiency estimation. Motor nameplate information was used in [4] to derive some estimation methods. Although these techniques are non-intrusive, they are not accurate enough. The standard equivalent-circuit method was mentioned in [5]. This technique required intrusive tests, including no-load, variable voltage, removed-rotor, and reverse rotation, so it is not feasible to apply this method for in-service systems. In [6,7], the last technique was modified to omit intrusive tests; however, these new algorithms need accurate motor parameters that may not be easy to obtain since some parameters, such as rotor and stator winding resistance, tend to change during motor operation. In [8–11] optimization techniques are used for efficiency estimation. These methods suffer from intrusive direct measurement of the stator winding resistance at ambient temperature.

There have been numerous studies on pump efficiency estimation methods in recent years, mainly based on the pump characteristic curves. Methods based on pump power consumption vs. flow rate (QP) and head vs. flow rate (QH) reported in [12] and a hybrid technique developed in [13] , estimate the operating point and the efficiency of centrifugal pumps. In [14] the characteristic curves are estimated based on the pump-specific speed and then these curves are used for hydraulic variables estimation. In [15], centrifugal pump characteristic curves are predicted based on a particle swarm

*Corresponding author's email: asadighi@ut.ac.ir

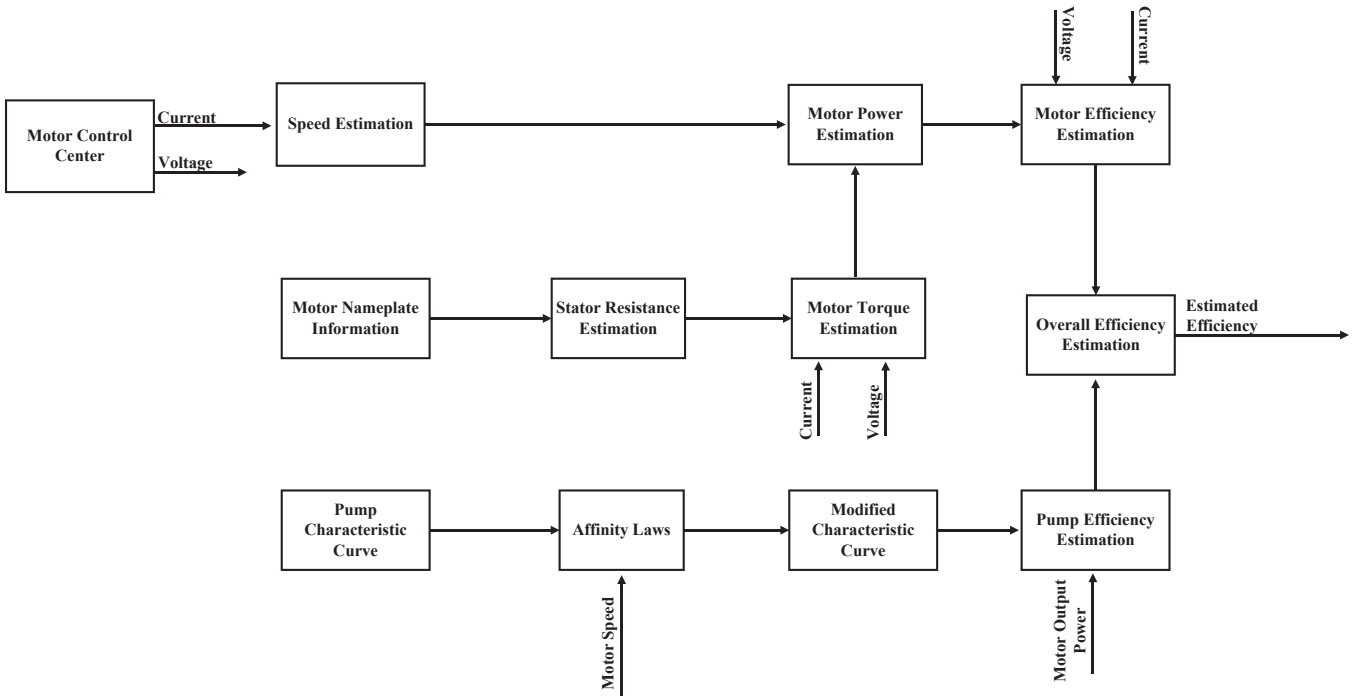

Fig. 1. The general approach for online efficiency estimation of an in-service pumping system.

optimization algorithm. In [16], pumping systems consisting of cascade centrifugal pumps and in [17], parallel pumps have been investigated. A method based on an interpolation algorithm on motor speed vs. motor shaft power curve is reported in [18]. This technique requires the measurement of motor speed and output power at different flow rates, and changing the flow rate is sometimes impossible for in-service systems. In all of these estimation techniques, the pump impeller speed and its input power are obtained by the variable frequency drive (VFD) used in the pumping system, so they cannot be implemented in systems where motors are not driven by this apparatus, or where the installed VFDs cannot estimate these quantities. Furthermore, the VFDs' estimated values have some errors since they usually come from the model-based algorithm that results in inaccurate operating points.

In [19–23], sensorless methods that use voltage and current to estimate mechanical variables such as speed and torque to control electric machines are investigated. The same techniques can also be employed to estimate the pumping system's efficiency. This paper introduces an online and non-intrusive algorithm that only needs voltage and current signals along with motor nameplate information and pump characteristic curves for efficiency estimation of induction-motor-driven centrifugal pumps. Regardless of whether the motor is powered by a VFD or not, this technique can be applied to all centrifugal pumps driven by three-phase induction motors, and this algorithm improves the accuracy of the estimated variables compared to the previous methods.

Fig. 1 shows an overview of the proposed algorithm. Section 2 is devoted to motor efficiency and output torque estimation, where a non-intrusive air-gap technique is discussed. In Section 3 stator resistance estimation method using motor nameplate information is presented. Next, Section 4 introduces a spectral analysis algorithm for rotor speed estimation. Finally, Section 5 explains the estimation of the pump operating point and its efficiency using input power and modified characteristic curves based on impeller rotational speed and affinity laws.

2- Motor Efficiency Estimation

Induction motor power flow is shown in Fig. 2. The input electric power transforms to air-gap power (electromagnetic power) on the stator side. Then on the rotor side, it converts to mechanical output power. According to Fig .2 for calculating the motor output power and efficiency, first, the air-gap power should be obtained, and then, converted power is determined based on the motor speed. Finally, by subtracting losses associated with friction and windage (P_{mech}) and also stray load on the rotor side ($P_{stray\ r}$), the output power is obtained.

Air-gap torque is the key to determine induction motor efficiency. Based on [24,25] this quantity can be calculated using motor line voltage, phase current, stator resistance, and

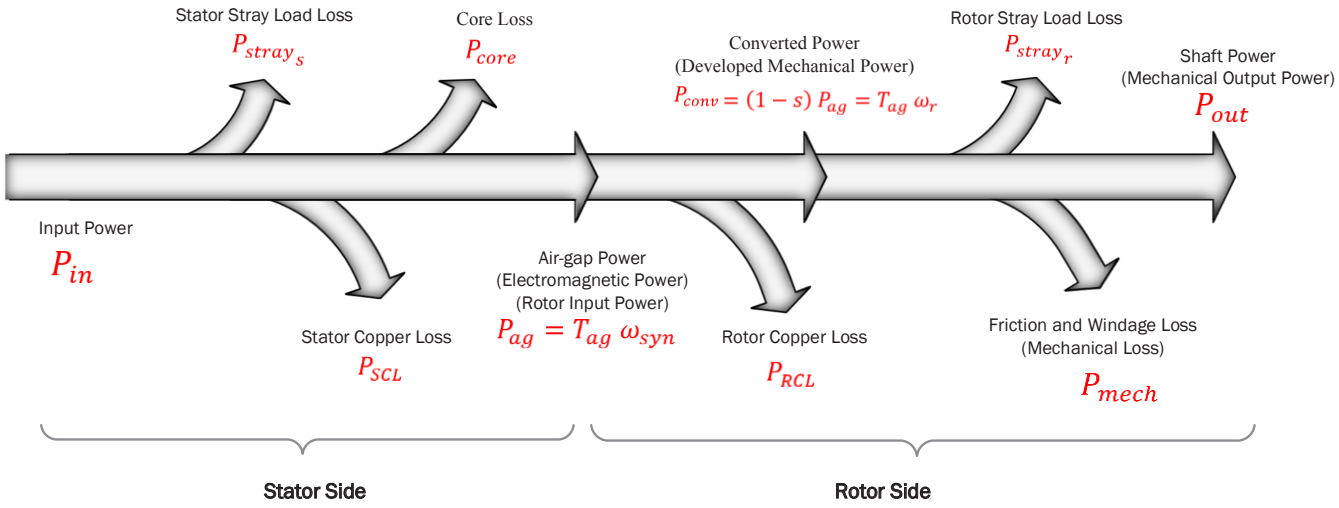

Fig. 2. Induction motor power flow.

Table 1. Stray load loss fraction at rated output power [5]

Rated Output Power (kW)	Stray Load Loss Fraction
0-90	0.018
91-375	0.015
376-1850	0.012
>1850	0.009

also motor nameplate information as the following equation:

$$T_{ag} = \frac{\sqrt{3}p}{3}\{(i_a - i_b)\cdot\int\left[v_{ca} + R_s\left(2i_a + i_b\right)\right]dt + (2i_a + i_b)\cdot\int\left[v_{ab} - R_s\left(i_a - i_b\right)\right]dt\} \quad (1)$$

Stator resistance is the only unknown parameter in (1), and its estimation algorithm is discussed in Section 3. It also should be noted that numeric methods like Simpson's rule can be used to calculate the integrals in (1).

As the rotor speed (ω_r) is estimated according to Section 4, the converted power can be calculated as:

$$P_{conv} = T_{ag}\,\omega_r \quad (2)$$

Next, the motor output power is obtained by subtracting the mentioned losses from the converted power as the following equation:

$$P_{out} = P_{conv} - P_{mech} - P_{stray_r} \quad (3)$$

The no-load test determines the value of these losses, but their estimations can be used instead to avoid this intrusive test. The mechanical loss is about 1.2% of the rated output power, and the stray load loss is estimated based on the rated output power multiplied by the associated fraction, summarized in Table. 1.

The motor input power is obtained using electrical quantities as:

$$P_{in} = mean\,(-v_{ca}(i_a + i_b) - v_{ab} i_b) \tag{4}$$

Finally, the motor efficiency can be calculated as:

$$\eta_{\text{motor}} = \frac{P_{out}}{P_{in}} \tag{5}$$

3- Stator Resistance Estimation

As reported in [26], direct measurement is the most accurate and straightforward way to determine stator winding resistance. However, this method is intrusive, and the obtained results are valid only for test temperature [27]. In [28–30], some model-based methods are introduced. These techniques need some motor equivalent-circuit parameters, including the magnetizing inductance and the rotor and stator leakage inductance with high accuracy, especially in the high-speed range [31]. DC signal injection is the other approach mentioned in [31]. Although this technique does not depend on motor parameters, provides accurate and reliable estimation for stator resistance, and takes temperature into account, it needs an extra electric circuit to be inserted into one phase of the motor and causes pulsation in torque and power dissipation. Some studies, such as [32–35], apply Fuzzy theory and neural networks to estimate stator resistance, but these methods need a command current signal and cannot be used for open-loop systems.

This paper estimates stator resistance through a non-intrusive approach mentioned in [36]. This algorithm is based on motor nameplate information and provides a simple way with acceptable accuracy that is sufficient for the energy auditing of these systems. The following nameplate information is required in this method:

rated output power (P_{out})
rated voltage (V_{rated})
rated current (I_{rated})
full load power factor (PF)
full load speed (N)
number of pole pairs (p)
supply frequency (f_1)

To obtain the stator resistance estimation, first, the input power and total loss at the rated condition should be calculated as mentioned below:

$$P_{in} = \sqrt{3}\, V_{rated} \cdot I_{rated} \cdot PF \tag{6}$$

$$P_{loss} = P_{in} - P_{out} \tag{7}$$

Then, apparent and reactive input powers are calculated as:

$$S_{in} = \frac{P_{in}}{PF} \tag{8}$$

$$Q_{in} = \sqrt{S_{in}^2 - P_{in}^2} \tag{9}$$

So the phasor input current is obtained as:

$$I_{phasor} = \frac{P_{in} - j\, Q_{in}}{V_{rated}} \tag{10}$$

The full load slip is calculated as:

$$s = 1 - \frac{N.p}{60\, f_1} \tag{11}$$

Next, the losses associated with stray load, mechanical, and core are estimated as fractions of the total loss and the rated output power.

$$P_{mech} = P_{loss} \cdot F_{mech} \tag{12}$$

$$P_{core} = P_{loss} \cdot F_{core} \tag{13}$$

$$P_{stray} = P_{out} \cdot F_{stray} \tag{14}$$

As discussed in [37], mechanical and core loss fractions can be considered to be about 0.14 and 0.12, respectively. stray load loss fraction can be obtained according to Table1 .

As mentioned in (15) and illustrated in Fig. 2, the converted power is the summation of output power, mechanical loss, and stray load loss on the rotor side.

$$P_{conv} = P_{out} + P_{mech} + P_{stray_r} \tag{15}$$

The air-gap power can be obtained as:

$$P_{ag} = \frac{P_{conv}}{1 - s} \tag{16}$$

According to Fig. 2, the stator copper loss can be calculated as:

$$P_{SCL} = P_{in} - P_{ag} - P_{core} \tag{17}$$

Finally, the stator resistance is obtained based on the following expression:

$$R_s = \frac{P_{SCL}}{|I_{phasor}|^2} \tag{18}$$

4- Rotor Speed Estimation

In [38–40], some model-based techniques for rotor speed estimation are investigated. These approaches provide a suitable estimate at high speed and are computationally cheap, meaning that they do not require more time or memory to solve than other techniques. But like other model-based methods needs accurate parameters for motor equivalent-circuit. Signal-based techniques consist of spectral signal analysis, and signal injection methods are the other estimation approaches. Frequency signal injection methods studied in [41–43] add a low or high-frequency signal to motor voltage. Since this signal interrupts the normal operation condition, these techniques are considered intrusive approaches and cannot be used for in-service systems. Spectral signal analysis is a non-intrusive approach for rotor speed estimation. It is based on particular harmonics in both voltage and current spectrum, provides accurate results, can be used for in-service systems in all load ranges, and does not depend on motor parameters [44]. Using a current signal for speed estimation is more common because current sensors are cheaper than voltage sensors and they usually found in motor control systems [38,45] In this paper spectral signal analysis method is used to determine rotor speed.

As discussed in [38], harmonics arise in the spectrum of current signals usually because of:

fundamental frequency;
winding distribution on the stator surface;
stator slots;
rotor slots;
air-gap eccentricity.

Among the mentioned harmonics, air-gap eccentricity and rotor slots are related to motor slip and can be used for rotor speed estimation. As mentioned in [40], calculated speeds from both methods are very close. However, the rotor slot harmonic algorithm is more complicated due to more parameters in this approach that should be identified first. So this paper focused on speed estimation based on air-gap eccentricity harmonics in current signals.

Air-gap eccentricity harmonics arise on both sides of the fundamental frequency due to motor design, installation issues, or bearing problems.

The motor slip and the eccentricity harmonic frequency are related through the following equation [40].

$$f_{\text{ecc}} = f_1 \left(1 \pm \left(\frac{1-s}{p}\right)\right) \tag{19}$$

Sometimes detecting the eccentricity harmonics may be challenging because they are close to fundamental frequency and have low amplitudes. Calculating the current spectrum with high resolution plays a crucial role in speed estimation since the accuracy of fundamental and eccentricity harmonics in the calculated spectrum determines the accuracy of the estimated speed.

The fast Fourier transform (FFT) is commonly used to calculate the spectrum. However, using this method alone is not usually enough, and some additional techniques, such as interpolation, zero padding, zoom, etc., are necessary to improve the resolution of the calculated spectrum, but it should be considered that applying each of these techniques increases computational cost. Another Fourier transform algorithm called chirp-Z transform (CZT) can calculate the spectrum in a specified frequency range. This technique provides a higher resolution for the calculated spectrum with the same sample points than the FFT algorithm [46]. Fewer sample points and the possibility to specify the frequency range make CZT a suitable replacement for FFT in the speed estimation algorithm.

Fig. 3 shows the proposed method for rotor speed estimation using eccentricity harmonics. First, the stator current is measured. Then, a low pass filter is used to prevent aliasing in the sampling step. As the current signal is sampled and collected, a Hanning window function is applied to reduce the leakage error. Next, the CZT technique is applied in the range of 0-80 Hz to find the fundamental harmonic. To increase the accuracy, the frequency range is limited to ±5 Hz around the obtained frequency in the previous step, and the CZT algorithm is applied again. Using the calculated frequency of fundamental harmonic and setting slip in the range of 0.001-0.07 in (19), a searching window in which the eccentricity harmonics are expected to be present is obtained. By applying the CZT technique in this frequency range, eccentricity harmonic is distinguished, and motor slip is calculated using (19) again. Then, rotor speed can be calculated as mentioned in [40].

$$N = \frac{60\, f_1\, (1-s)}{p} \tag{20}$$

5- Pump Efficiency Estimation

The proposed method to estimate the pump operating point and efficiency is based on characteristic curves consisting of pump power consumption vs. flow rate (QP) and head vs. flow rate (QH) as discussed in the following. Note that this technique is only applicable to centrifugal

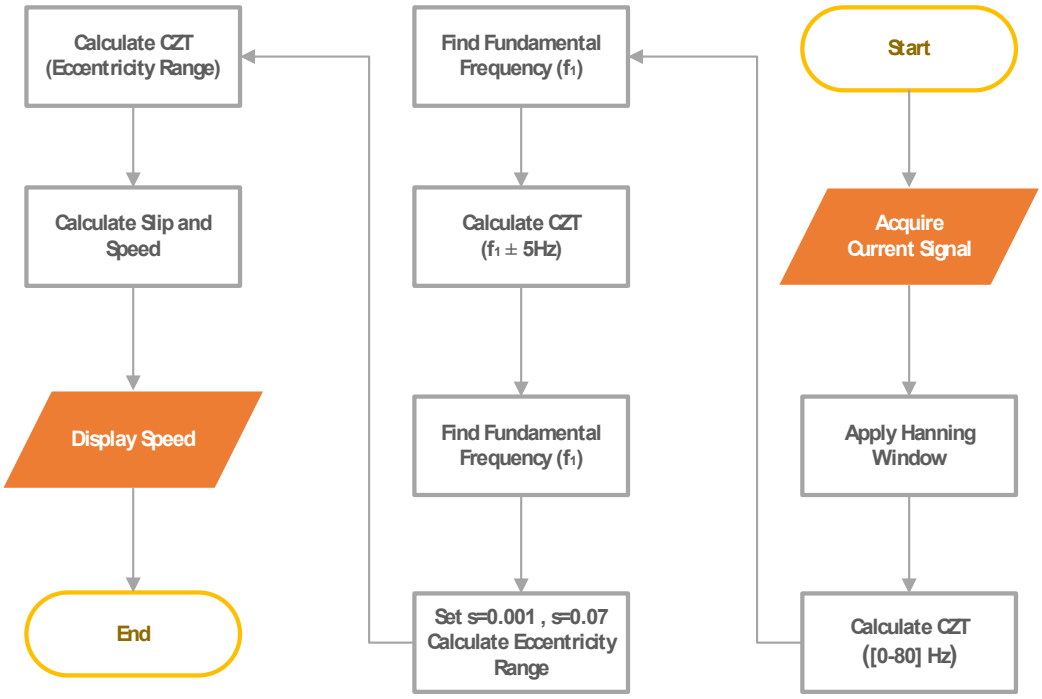

Fig. 3. Speed estimation algorithm using eccentricity harmonics.

pumps driven by three-phase induction motors. Therefore, the impeller rotational speed of the pump can be estimated using the algorithm given in Section 4, assuming it is equal to the induction motor rotor speed. Also, the pump input and motor output power are considered equal and can be estimated using the discussed approach in Section 2.

As the pump characteristic curves report at nominal speed, and the operating point estimation algorithm requires these curves at instantaneous speed, affinity laws mentioned in [47] are used to modify them as:

$$\frac{Q}{Q_{\text{nom}}} = \frac{N}{N_{\text{nom}}} \tag{21}$$

$$\frac{H}{H_{nom}} = \left(\frac{N}{N_{nom}}\right)^2 \tag{22}$$

$$\frac{P}{P_{\text{nom}}} = \left(\frac{N}{N_{\text{nom}}}\right)^3 \tag{23}$$

As illustrated in Fig.4 the pump flow rate is estimated by the intersection of the motor output power and modified QP curve. Then, according to Fig. 5, the pump head is determined by the intersection of the obtained flow rate and modified QH curve [12].

As the pump flow rate and head are estimated, the efficiency can be calculated based on fluid density as mentioned in [47].

$$\eta_{pump} = \frac{\rho g H Q}{(P_{in})_{pump}} \tag{24}$$

The rotational speed affects the estimated results obtained from this algorithm. As reported in [13], the allowable deviation is about 20% of the pump nominal speed, meaning that the accuracy decreases out of this range, and the proposed method is not valid anymore. Also, as discussed in [41], this method failed in some abnormal operating conditions, such as flow recirculation or cavitation.

Since the estimation algorithm is based on the characteristic curves, the accuracy of the obtained results is highly dependent on the accuracy of these curves. On the other hand, the published curves have some errors and are different from the actual ones. As suggested in [12], the QP curve can be corrected by closing the discharge valve, calculating the pump input power, and moving the entire curve according to this obtained value. This technique significantly improves

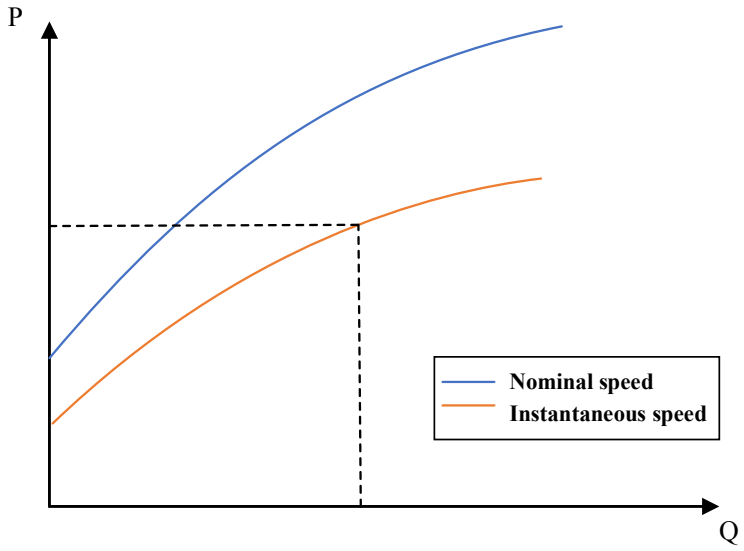

Fig. 4. Flow rate estimation using QP curve.

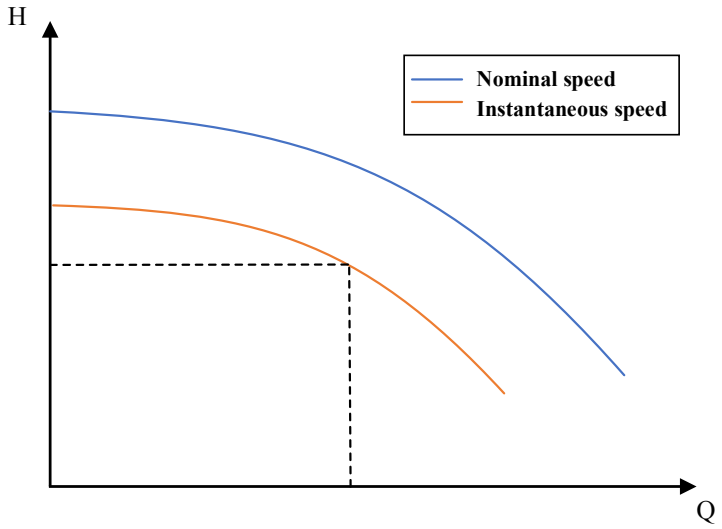

Fig. 5. Head estimation using QH curve.

the QP curves.

The shape of QP curves is also important in this algorithm, and these curves should have a sufficient slope. Fig.6 illustrates that a little shift in input power changes the flow rate significantly in QP curves with a gentle slope.

Another proposed method for pump operating point estimation is based on the hydraulic system process curve. This curve represents the relationship between the flow rate and the process head. As shown in Fig.7 the process head comprises static and dynamic head parts. The static part expresses the fluid vertical lift, and the dynamic head describes the losses associated with piping, valves, fittings, enlargements, contractions, etc., in the hydraulic system.

The process curve can be expressed using a second-order polynomial as:

$$H_{\text{process}} = a + b\,Q^2 \tag{25}$$

External measurement of static and dynamic heads in the hydraulic system is the general approach for determining parameters a and b in (25).

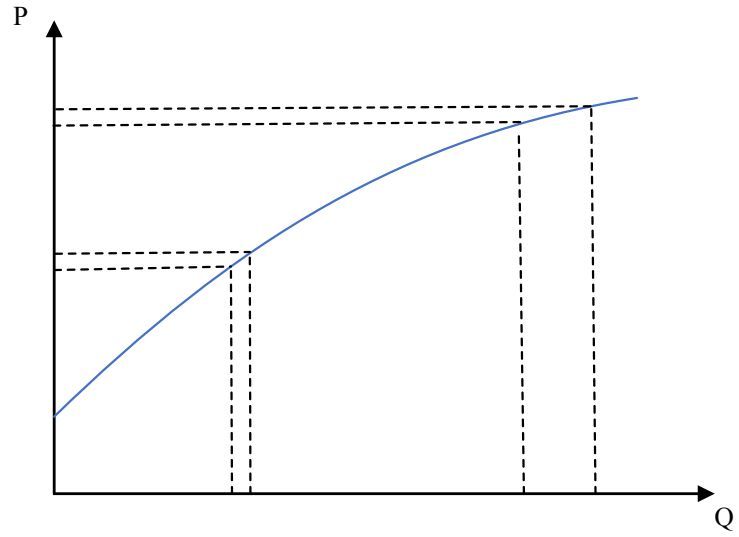

Fig. 6. The effect of QP curve slope in the estimation algorithm.

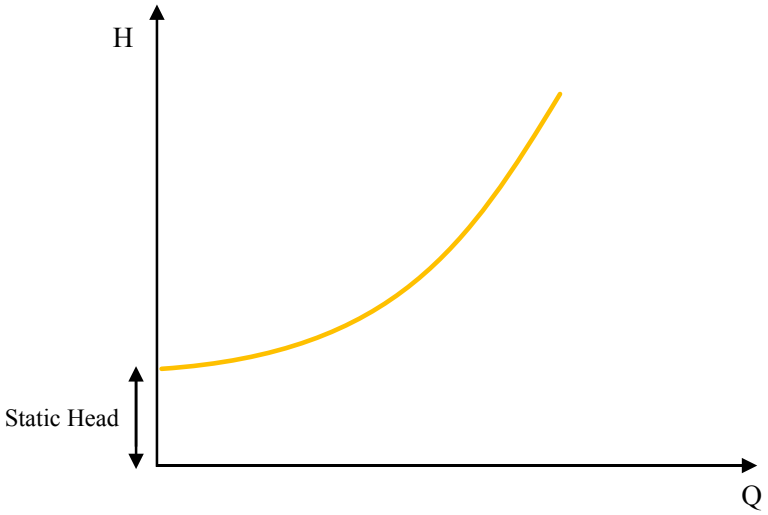

Fig. 7. The process curve of a hydraulic system.

Using variable frequency drive (VFD) to adjust the rotational speed is one of the most efficient and popular techniques for flow rate control. Under this condition, parameters in (25) do not change so much and can be identified using the least square algorithm and the QP algorithm for some operating points at steep areas of this curve. As the static head (a) and dynamic coefficient (b) of the process curve are identified, the flow rate and head can be estimated by the intersection of the modified QH curve and obtained process curve, as illustrated in Fig.8. As the process curve is obtained, this hybrid algorithm can be a suitable substitution for the previous method to estimate the pump operating point, especially when the slope of the QP curve is not steep enough.

6- Experimental Results

6- 1- Motor- generator setup

To test and verify the proposed algorithms for speed and motor power estimation, an experimental setup, shown in Fig. 9 was designed and built. This setup consists of a 1.5-kW SIEMENS induction motor (1AV1094B) fed by a three-phase PENTAX (DSI-400-2k2G3-00) variable frequency drive, a LENZ dc generator (GN-100), and a resistor bank to

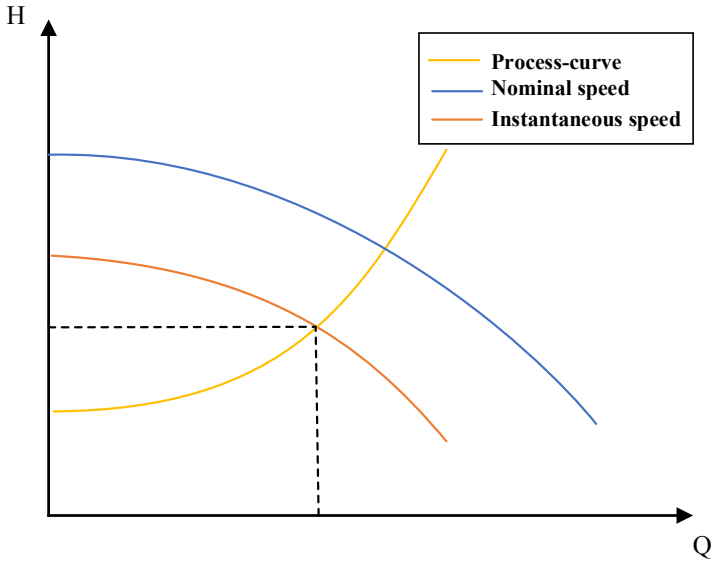

Fig. 8. Head estimation applying the QH algorithm.

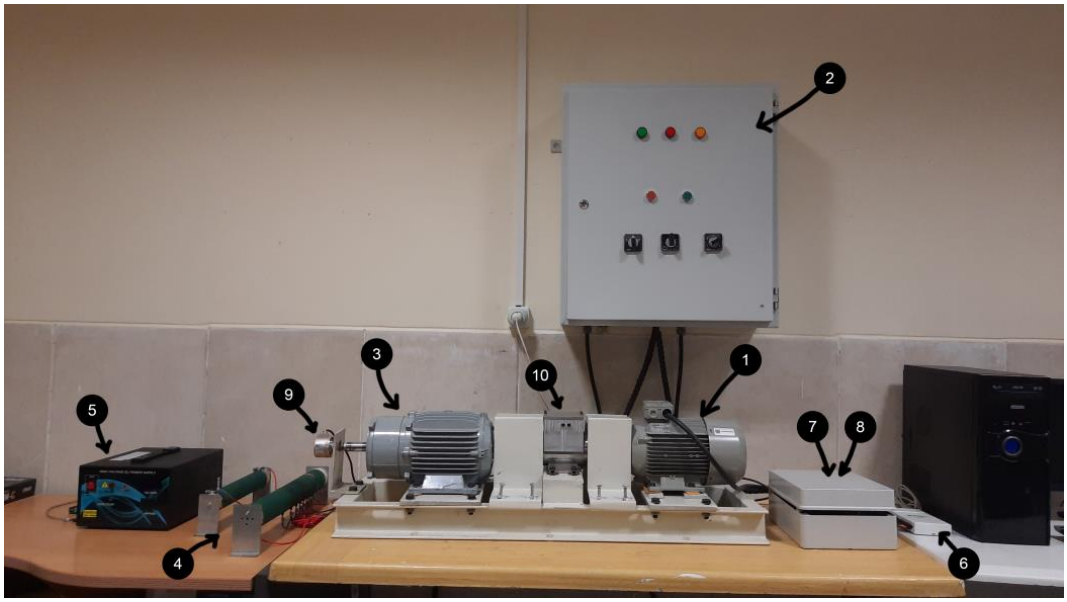

Fig. 9. Motor-Generator experimental setup.

dissipated the generated power. The motor supply frequency and mechanical load can be adjusted using the mentioned VFD and varying the resistance connected to the generator. A TS1 torque transducer is coupled to the induction motor and generator for direct measurement of output torque. Also, an OPKON encoder (PSI50SH) enables rotor speed measurement. An electric board consisting of three LEM voltage transducers (LV25-P), three LEM current transducers (LA55-P), and an eight-order Chebyshev anti-aliasing filter is used to measure the phase signals and prepare them to be sampled. An NI data acquisition board (USB-6210) samples the voltage and current signals at 8-kHz rate. Fig. 10 illustrates the schematic of this test setup.

Fig. 11 shows the eccentricity harmonics in the calculated spectrum of the current signal when the fundamental frequency is about 36 Hz.

Fig. 12 compares the estimated rotor speed obtained by the eccentricity harmonic approach with encoder results in some operating points. The maximum relative error obtained for this estimation technique is about 0.6%. Therefore, this method is accurate and can be considered a suitable substitute for encoders.

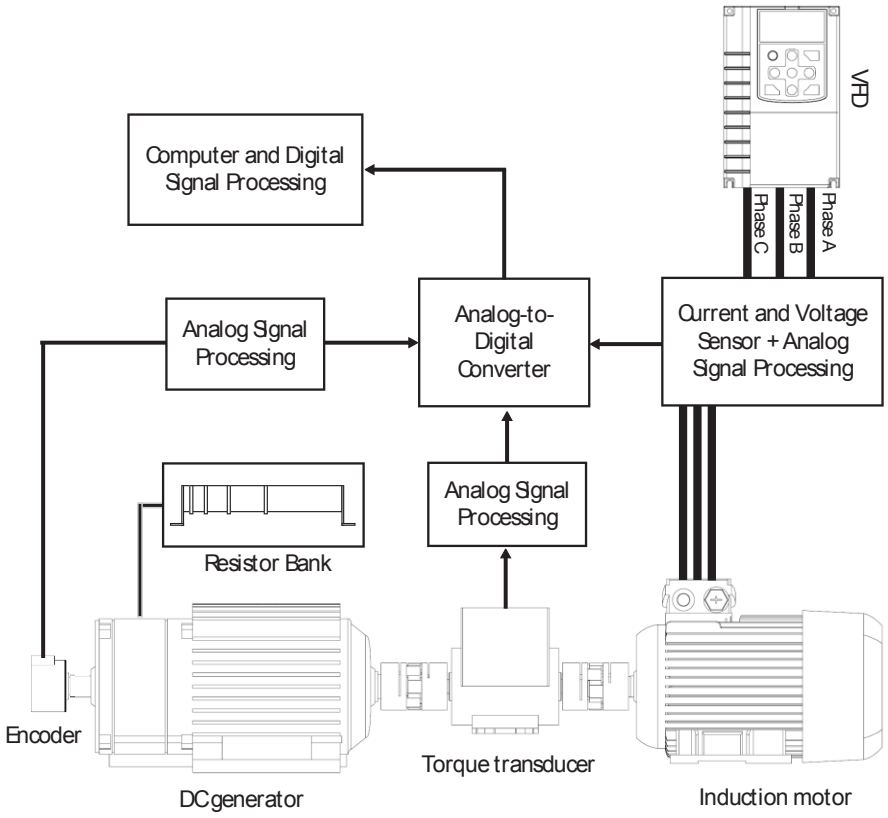

Fig. 10. The Schematic of Motor-Generator setup.

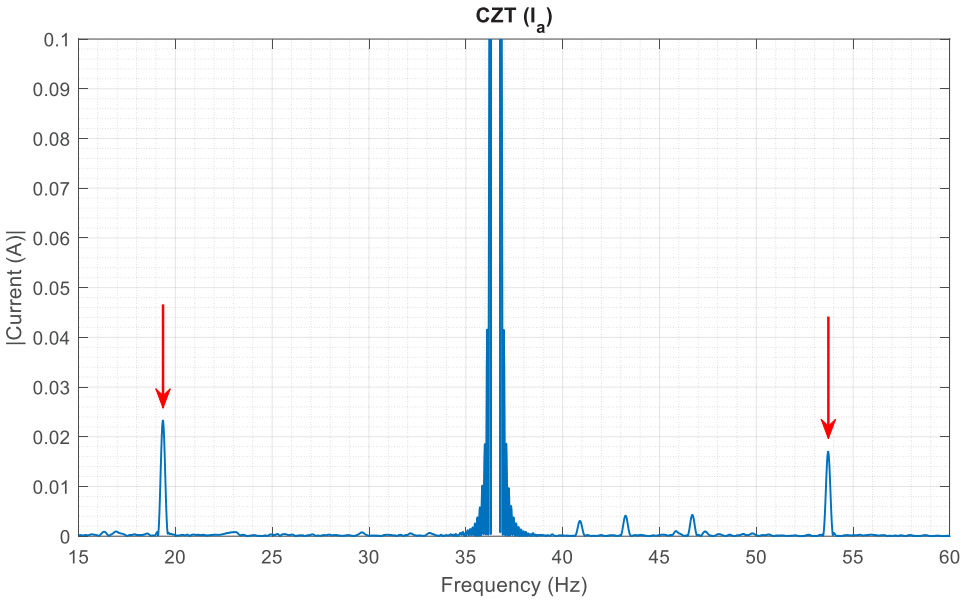

Fig. 11. Eccentricity harmonic in the calculated current signal spectrum.

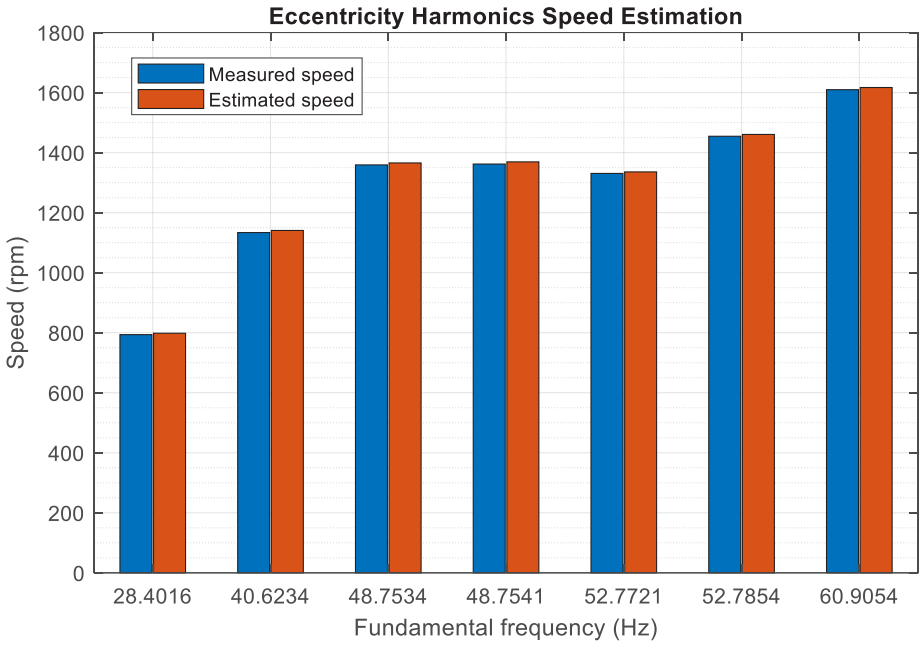

Fig. 12. Speed estimation using eccentricity harmonic technique in Motor-Generator setup.

Table 2. Motor nameplate information.

Parameter	Value
Power (kW)	1.5
Frequency (Hz)	50
Speed (rpm)	1410
Pawer factor	0.8
Voltage (V)	230/400 (Δ/Y)
Current (A)	6.1/3.35 (Δ/Y)

As discussed before, stator resistance is required to estimate motor output torque and its efficiency. Using motor nameplate information which is summarized in Table. 2, and the proposed algorithm, this parameter was estimated as 5.0592 Ù, while its actual value obtained by direct measurement was 5.8250 Ù.

The motor output power estimation algorithm mentioned in Section 1 was also tested in this setup at four operating points that defined the 45% (OP4), 65% (OP3), 80% (OP2), and 100% (OP1) of rated output power. Fig. 13 shows the estimated output power against the actual one obtained by measured output torque multiplied by measured rotational speed. This figure shows the input power as well.

According to Fig. 13, the accuracy of the estimation technique is reduced by moving away from the rated condition, as the relative estimation error at operating point 1 is 0.8%, and it increases to 7.5% at operating point 4.

6- 2- Laboratory Pumping System

A test bench in the turbo machinery laboratory was used to verify the pump operating point and its efficiency estimation techniques. Fig.14 shows this setup which comprises an

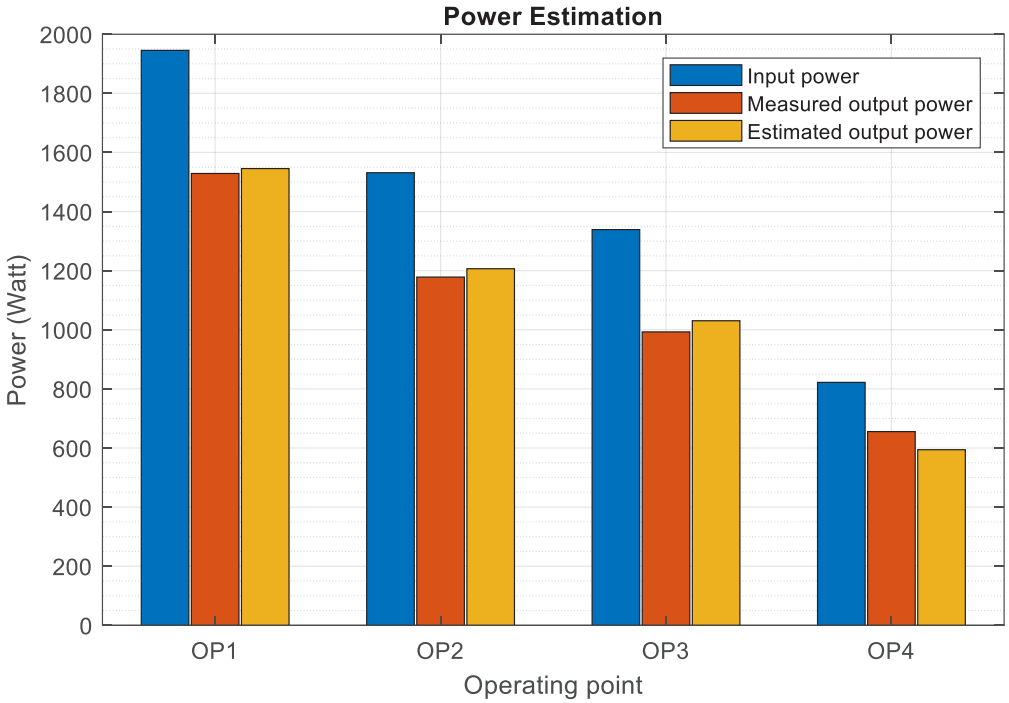

Fig. 13. Power estimation for Motor-Generator setup.

Fig. 14. Pumping system experimental setup.

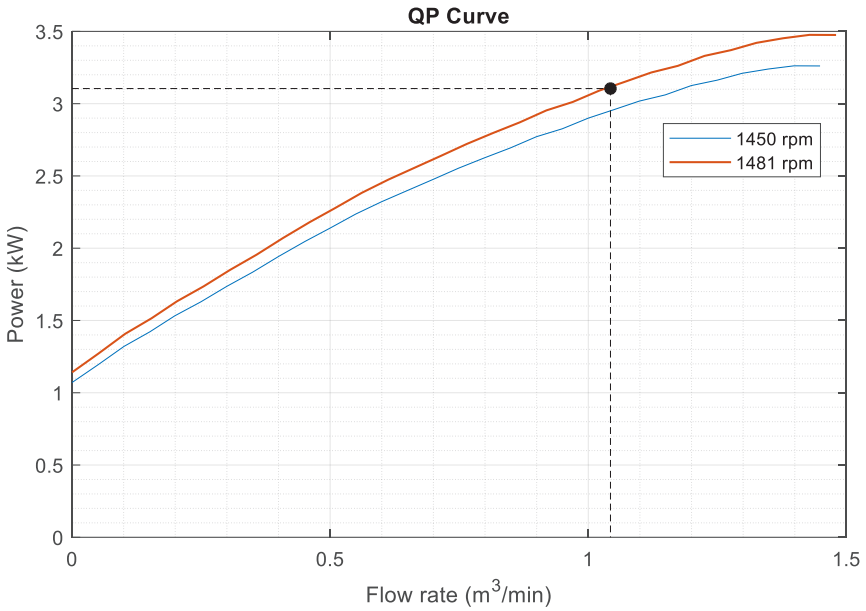

Fig. 15. Flow rate estimation based on modified QP curve.

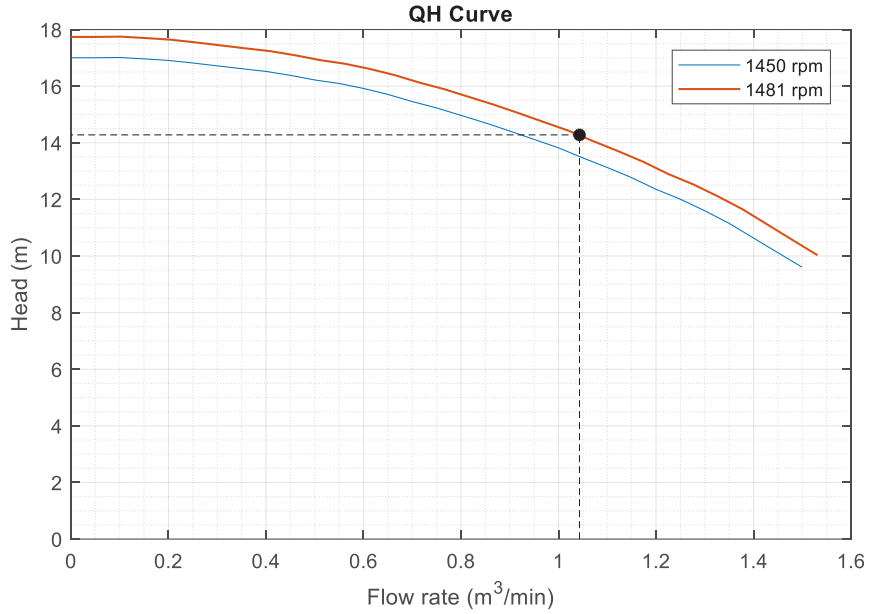

Fig. 16. Pump head estimation based on modified QH curve.

11-kW three-phase induction motor (VEM) coupled to an EBARA centrifugal pump ($1000\times80FS$). The fluid flow rate is measured using FARASANG ABZAR electromagnetic flowmeter (MF300), the head is obtained using two TG1 barometers installed in the inlet and outlet of the pump, and the data collection board is the same as the previous setup.

The estimation algorithm was implemented on this setup at five operating points, which correspond to the flow rate of 17.4 (OP1), 14 (OP2), 10.5 (OP3), 7 (OP4), and 3.5 (OP5) liters per second.

Fig. 15 and Fig. 16 show the proposed method for flow rate and head estimation at operating point 1, where the estimated motor speed and output power were 1481 rpm and 3.1047 kW.

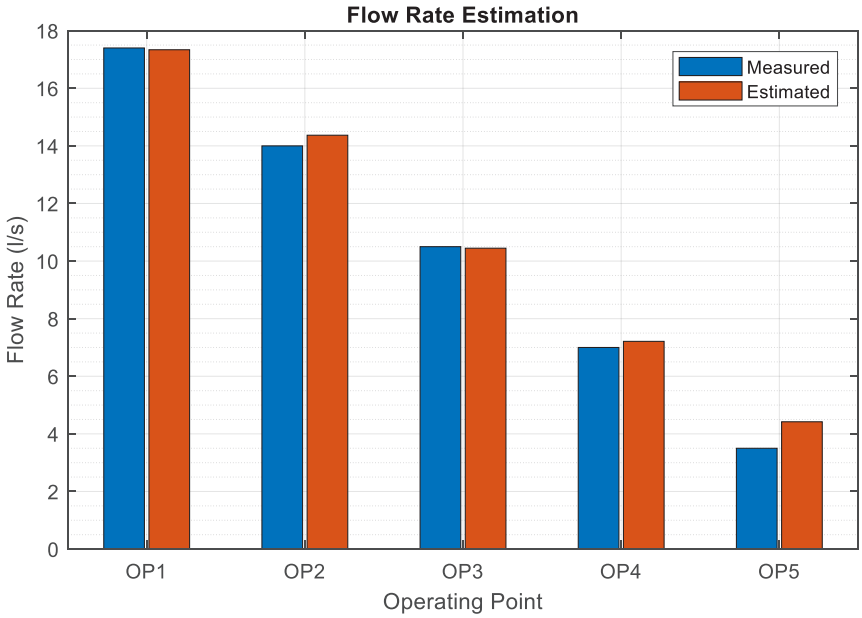

Fig. 17. Flow rate estimation for the pumping setup.

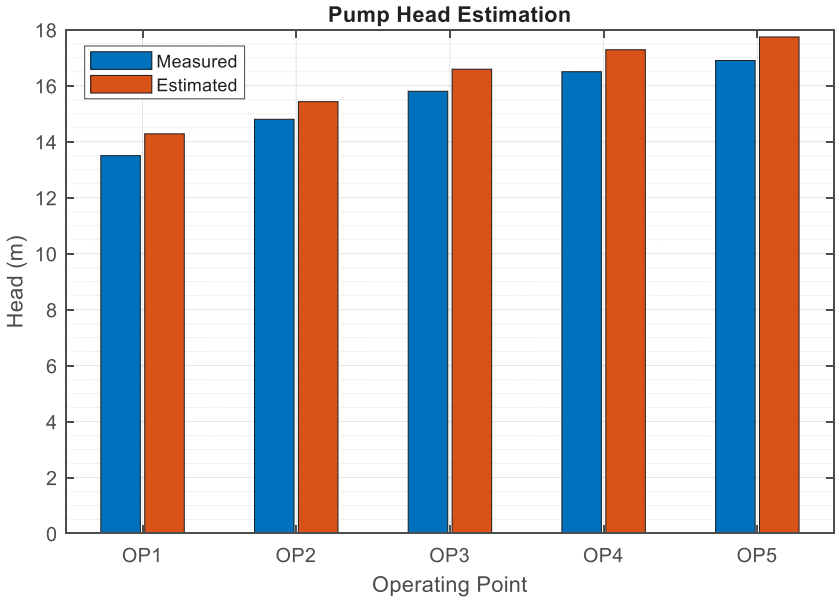

Fig. 18. Pump head estimation for the pumping setup.

Fig. 17 compares the estimated flow rate with the direct measurement at mentioned operating points. This figure shows that the estimation accuracy decreases as the pump operating point drifts from the best efficiency point (OP1). The maximum relative error is about 26.3%, but it reduces to 0.3% at OP1.

Fig. 18 demonstrates the estimated and measured pump head at the discussed operating point. The maximum relative error for head estimation is 5.7%.

Fig. 19 compares the estimated pump efficiency with the actual one at operating point 1 to operating point 5.

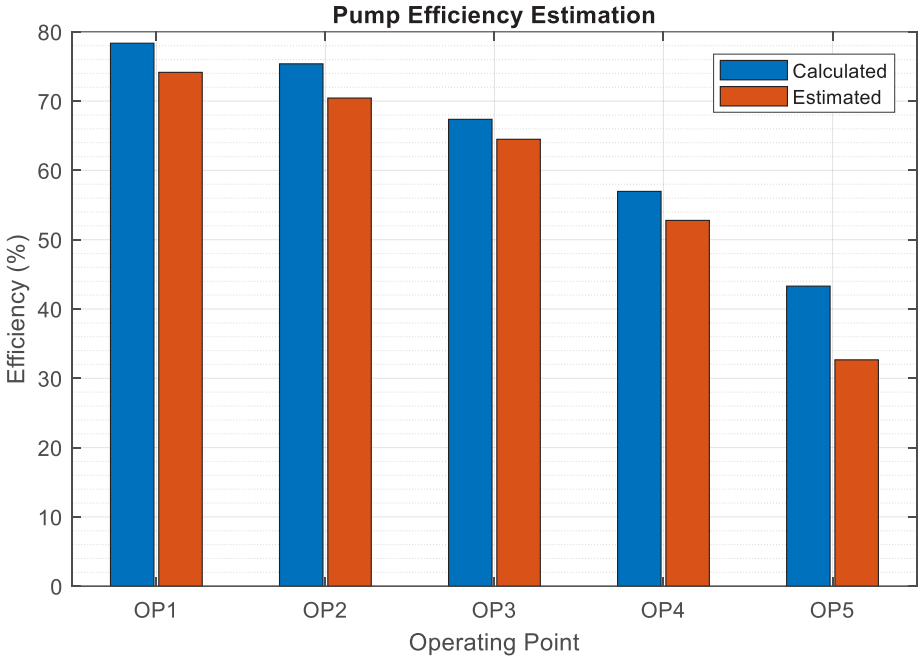

Fig. 19. Efficiency estimation for pumping system setup.

7- Nomenclature

f_1	Fundamental supply frequency, Hz	P_{mech}	Mechanical load loss, W
f_{ecc}	Eccentricity harmonic frequency, Hz	P_{SCL}	Stator copper loss, W
g	Gravitational acceleration, $m.s^{-2}$	P_{stray}	Stray loss, W
H	Pump head, m	Q	Pump flow rate, $m^3.s^{-1}$
i_a, i_b, i_c	Line current, A	Q_{in}	Reactive input power. $V.A$
I_{phasor}	Phasor input current, A	R_s	Stator resistance, Ω
I_{rated}	Rated current, A	s	Slip
N	Rotational speed, (rpm)	S_{in}	Apparent input power, $V.A$
p	Pole pairs number	T_{ag}	Air-gap torque, $N.m$
P	Power, W	v_{ab} , v_{bc} , v_{ca}	Line voltage, V
P_{ag}	Air-gap power, W	V_{rated}	Rated voltage, V
P_{conv}	Converted power, W	η	Efficiency
P_{core}	Core loss, W	ρ	Fluid density, $kg.m^{-3}$
PF	Power factor	ω_r	Rotor speed, $rad \cdot s^{-1}$
P_{loss}	Total loss, W		

8- Conclusion

This paper proposed an online non-intrusive approach for estimating the operating point and efficiency of a pumping system consisting of centrifugal pumps and three-phase induction motors. Since the mentioned algorithm needs rotor speed and stator resistance, these values were estimated using eccentricity harmonics in the calculated spectrum of current signal and motor nameplate information. Also, an air-gap technique was used to estimate motor output power. The pump head and flow rate were estimated using a hybrid method based on characteristic curves. Finally, a motor generator and pumping laboratory setups were introduced, and all the mentioned methods were implemented and verified experimentally. The obtained results showed the ability of the proposed approach to estimate the efficiency of the whole motor pump chain in a non-intrusive way with acceptable accuracy only by using motor voltage and current signals and its nameplate information along with pump characteristic curves.

References

[1] Abdelaziz EA, Saidur R, Mekhilef S. A review on energy saving strategies in industrial sector. Renew Sustain Energy Rev 2011;15:150–68. https://doi.org/10.1016/j.rser.2010.09.003.

[2] Chuan W, Xiaoke H, Desheng Z, Bo H. Numerical and experimental study of the self-priming process of a multistage self-priming centrifugal pump. Energy Res 2019:1–19.

[3] Ahonen T, Kortelainen JT, Tamminen JK, Ahola J. Centrifugal pump operation monitoring with motor phase current measurement. Int J Electr Power Energy Syst 2012;42:188–95. https://doi.org/10.1016/j.ijepes.2012.04.013.

[4] Lu B, Habetler TG, Harley RG. A survey of efficiency-estimation methods for in-service induction motors. IEEE Trans Ind Appl 2006;42:924–33. https://doi.org/10.1109/TIA.2006.876065.

[5] IEEE Standard Test Procedure for Polyphase Induction Motors and Generators. IEEE Stand 112-2004, Nov 2004 2004.

[6] El-Ibiary Y. An Accurate Low-Cost Method for Determining Electric Motors' Efficiency for the Purpose of Plant Energy Management. IEEE Trans Ind Appl 2003;39:1205–10. https://doi.org/10.1109/TIA.2003.813686.

[7] Hsu JS, Kueck JD, Olszewski M, Casada DA, Otaduy PJ, Tolbert LM. Comparison of induction motor field efficiency evaluation methods. IEEE Trans Ind Appl 1998;34:117–25. https://doi.org/10.1109/28.658732.

[8] Bijan MG, Pillay P. Efficiency estimation of the induction machine by particle swarm optimization using rapid test data with range constraints. IEEE Trans Ind Electron 2019;66:5883–94. https://doi.org/10.1109/TIE.2018.2873121.

[9] Mutluer M, Bilgin O. Application of a hybrid evolutionary technique for efficiency determination of a submersible induction motor. Turkish J Electr Eng Comput Sci 2011;19:877–90. https://doi.org/10.3906/elk-1003-428.

[10] Gómez JR, Quispe EC, De Armas MA, Viego PR. Estimation of induction motor efficiency in-situ under unbalanced voltages using genetic algorithms. Proc 2008 Int Conf Electr Mach ICEM'08 2008:25–8. https://doi.org/10.1109/ICELMACH.2008.4799965.

[11] Phumiphak T, Chat-Uthai C. Estimation of induction motor parameters based on field test coupled with genetic algorithm. PowerCon 2002 - 2002 Int Conf Power Syst Technol Proc 2002;2:1199–203. https://doi.org/10.1109/ICPST.2002.1047592.

[12] Ahonen T, Tamminen J, Ahola J, Viholainen J, Aranto N, Kestilä J. Estimation of pump operational state with model-based methods. Energy Convers Manag 2010;51:1319–25. https://doi.org/10.1016/j.enconman.2010.01.009.

[13] Ahonen T, Tamminen J, Ahola J, Kestilä J. Frequency-converter-based hybrid estimation method for the centrifugal pump operational state. IEEE Trans Ind Electron 2012;59:4803–9. https://doi.org/10.1109/TIE.2011.2176692.

[14] Pöyhönen S, Ahonen T, Ahola J, Punnonen P, Hammo S, Nygren L. Specific speed-based pump flow rate estimator for large-scale and long-term energy efficiency auditing. Energy Effic 2019;12:1279–91. https://doi.org/10.1007/s12053-018-9751-4.

[15] [15] Luo H, Zhou P, Shu L, Mou J, Zheng H, Jiang C, et al. Energy Performance Curves Prediction of Centrifugal Pumps Based on Constrained PSO-SVR Model. Energies 2022;15:1–19. https://doi.org/10.3390/en15093309.

[16] Arun AS, Subramaniam U, Madurai Elavarasan R, Raju K, Shanmugam P. Sensorless parameter estimation of VFD based cascade centrifugal pumping system using automatic pump curve adaption method. Energy Reports 2021;7:453–66. https://doi.org/10.1016/j.egyr.2021.01.002.

[17] Arun Shankar VK, Umashankar U, Paramasivam S, Hanigovszki N. An Energy Efficient Control Algorithm for Parallel Pumping Industrial Motor Drives System. Proc 2018 IEEE Int Conf Power Electron Drives Energy Syst PEDES 2018 2018:1–6. https://doi.org/10.1109/PEDES.2018.8707618.

[18] Wu Y, Wu D, Fei M, Xiao G, Gu Y, Mou J. The Estimation of Centrifugal Pump Flow Rate Based on the Power–Speed Curve Interpolation Method. Processes 2022;10:2163. https://doi.org/10.3390/pr10112163.

[19] Sadighi A, Kim W. Adaptive-Neuro-Fuzzy-Based Sensorless Control of a Smart-Material Actuator 2011;16:371–9.

[20] Chi S, Zhang Z, Xu L. Sliding-mode sensorless control of direct-drive PM synchronous motors for washing machine applications. IEEE Trans Ind Appl 2009;45:582–

90. https://doi.org/10.1109/TIA.2009.2013545.

[21] Genduso F, Miceli R, Rando C, Galluzzo GR. Back EMF sensorless-control algorithm for high-dynamic performance PMSM. IEEE Trans Ind Electron 2010;57:2092–100. https://doi.org/10.1109/TIE.2009.2034182.

[22] Chen Z, Tomita M, Doki S, Okuma S. An extended electromotive force model for sensorless control of interior permanent-magnet synchronous motors. IEEE Trans Ind Electron 2003;50:288–95. https://doi.org/10.1109/TIE.2003.809391.

[23] Wang X, Kennel R, Ma Z, Gao J. Analysis of permanent-magnet machine for sensorless control based on high-frequency signal injection. Conf Proc - 2012 IEEE 7th Int Power Electron Motion Control Conf - ECCE Asia, IPEMC 2012 2012;4:2367–71. https://doi.org/10.1109/IPEMC.2012.6259225.

[24] Lu B, Habetler TG, Harley RG. A nonintrusive and in-service motor-efficiency estimation method using air-gap torque with considerations of condition monitoring. IEEE Trans Ind Appl 2008;44:1666–74. https://doi.org/10.1109/TIA.2008.2006297.

[25] Hsu (Htsui) JS. Monitoring of defects in induction motors through air-gap torque observation. IEEE Trans Energy Convers 1995;31:1016–21.

[26] Andrus WE, Duncan RO, Flint CW, Moore V a, Barber M. IEEE Std 118TM-1978 (Withdrawn 2005) Standard Test Code for Resistance Measurement 1992;1978.

[27] Cheng S, Du Y, Restrepo JA, Zhang P, Habetler TG. A nonintrusive thermal monitoring method for induction motors fed by closed-loop inverter drives. IEEE Trans Power Electron 2012;27:4122–31. https://doi.org/10.1109/TPEL.2012.2188045.

[28] Habetler TG, Harley RG, Gritter DJ. A Stator and Rotor Resistance Estimation Technique for Conductor Temperature Monitoring. Ind Appl Conf 2000:381–7.

[29] Zhen L, Xu L. Sensorless field orientation control of induction machines based on a mutual MRAS scheme. IEEE Trans Ind Electron 1998;45:824–31. https://doi.org/10.1109/41.720340.

[30] [30] Deng A, Zou J, Shao Z, Huang G, Shi L, Deng W. Improvement on asynchronous motor system identification based on interactive MRAS. Proc 2015 27th Chinese Control Decis Conf CCDC 2015 2015:448–53. https://doi.org/10.1109/CCDC.2015.7161734.

[31] Lee S Bin, Habetler TG. An online stator winding resistance estimation technique for temperature monitoring of line-connected induction machines. IEEE Trans Ind Appl 2003;39:685–94. https://doi.org/10.1109/TIA.2003.811789.

[32] Karanayil B, Rahman MF, Grantham C. Online stator and rotor resistance estimation scheme using artificial neural networks for vector controlled speed sensorless induction motor drive. IEEE Trans Ind Electron 2007;54:167–76. https://doi.org/10.1109/TIE.2006.888778.

[33] Zinger DS, Elbuluk ME, Mir S. PI and fuzzy estimation for the stator resistance in direct torque control of induction machines 1994.

[34] Cabrera LA, Elbuluk ME. Tuning the stator resistance of induction motors using artificial neural network. PESC Rec - IEEE Annu Power Electron Spec Conf 1995;1:421–7. https://doi.org/10.1109/PESC.1995.474845.

[35] Bose BK, Patel NR. Quasi-fuzzy estimation of stator resistance of induction motor. IEEE Trans Power Electron 1998;13:401–9. https://doi.org/10.1109/63.668097.

[36] Lee K, Frank S, Sen PK, Polese LG, Alahmad M, Waters C. Estimation of induction motor equivalent circuit parameters from nameplate data. 2012 North Am Power Symp NAPS 2012 2012. https://doi.org/10.1109/NAPS.2012.6336384.

[37] Saidur R. A review on electrical motors energy use and energy savings. Renew Sustain Energy Rev 2010;14:877–98. https://doi.org/10.1016/j.rser.2009.10.018.

[38] Aiello M, Cataliotti A. An Induction Motor Speed Measurement Method Based on Current Harmonic Analysis With the Chirp-Z Transform. IEEE Trans Instrum Meas VOL 54, NO 5 Oct 2005 2005.

[39] Bharadwaj RM, Parlos AG. Neural state filtering for adaptive induction motor speed estimation. Mech Syst Signal Process 2003;17:903–24. https://doi.org/10.1006/mssp.2002.1523.

[40] Hurst KD, Habetler TG. Sensorless Speed Measurement Using Current Harmonic Spectral Estimation in Induction Machine Drives. Electronics 1996;11.

[41] Hammo S, Viholainen J. Testing the accuracy of pump flow calculation without metering. World Pumps 2005;2005:36–9. https://doi.org/10.1016/S0262-1762(05)70846-4.

[42] Hinkkanen M, Leppänen VM, Luomi J. Flux observer enhanced with low-frequency signal injection allowing sensorless zero-frequency operation of induction motors. IEEE Trans Ind Appl 2005;41:52–9. https://doi.org/10.1109/TIA.2004.840958.

[43] Holtz J. Sensorless control of induction machines - With or without signal injection? IEEE Trans Ind Electron 2006;53:7–30. https://doi.org/10.1109/TIE.2005.862324.

[44] Bane P, Veran V, Boris D, Dragan M, Nikola V. Rotor slot harmonics based induction machine speed estimation. Int Symp Power Electron 2017.

[45] Arabaci H. A genetic algorithm approach for sensorless speed estimation by using rotor slot harmonics. Lect Notes Eng Comput Sci 2015;2219:265–9.

[46] Martin G. Chirp Z-Transform Spectral Zoom Optimization with MATLAB. Sandia Natl Lab Rep SAND2005-7084 2005.

[47] Pritchard PJ, Mitchell JW. Fox and McDonald's Introduction to Fluid Mechanics. 9th ed. John Wiley & Sons; 2016.

HOW TO CITE THIS ARTICLE

M. J. Karimi, A. Sadighi, Online Non-Intrusive Efficiency Monitoring of Pumping Systems. AUT J. Elec. Eng., 56(1) (Special Issue) (2024) 19-36.

DOI: 10.22060/ajme.2020.16761.5832